

Prediction of scandium tetraboride from first-principles calculations: Crystal structures, phase stability, mechanical properties,and hardness

Bin-Hua Chu(初斌华)† and Yuan Zhao(赵元)

Citation: Chin. Phys. B, 2021, 30 (**7**): 076107. DOI: 10.1088/1674-1056/abe116
Journal homepage: http://cpb.iphy.ac.cn; http://iopscience.iop.org/cpb

What follows is a list of articles you may be interested in

Ground-state structure and physical properties of YB_3 predicted from first-principles calculations

Bin-Hua Chu(初斌华), Yuan Zhao(赵元), and De-Hua Wang(王德华)
Chin. Phys. B, 2021, 30 (**4**): 046101. DOI: 10.1088/1674-1056/abcf94

Ab initio study on crystal structure and phase stability of ZrC_2 under high pressure

Yong-Liang Guo(郭永亮), Jun-Hong Wei(韦俊红), Xiao Liu(刘潇), Xue-Zhi Ke(柯学志), and Zhao-Yong Jiao(焦照勇)
Chin. Phys. B, 2021, 30 (**1**): 016101. DOI: 10.1088/1674-1056/abb3e7

Effects of Re, Ta, and W in [110] (001) dislocation core of γ/γ' interface to Ni-based superalloys: First-principles study

Chuanxi Zhu(朱传喜), Tao Yu(于涛)
Chin. Phys. B, 2020, 29 (**9**): 096101. DOI: 10.1088/1674-1056/abad26

Tunable electronic structures of germanane/antimonene van der Waals heterostructures using an external electric field and normal strain

Xing-Yi Tan(谭兴毅), Li-Li Liu(刘利利), Da-Hua Ren(任达华)
Chin. Phys. B, 2020, 29 (**7**): 076102. DOI: 10.1088/1674-1056/ab8a39

Theoretical study on martensitic-type transformation path from rutile phase to α-PbO_2 phase of TiO_2

Wen-Xuan Wang(王文轩), Zhen-Yi Jiang(姜振益), Yan-Ming Lin(林彦明), Ji-Ming Zheng(郑继明), Zhi-Yong Zhang(张志勇)
Chin. Phys. B, 2020, 29 (**7**): 076101. DOI: 10.1088/1674-1056/ab8abe

---

Prediction of scandium tetraboride from first-principles calculations: Crystal structures, phase stability, mechanical properties, and hardness*

Bin-Hua Chu(初斌华)† and Yuan Zhao(赵元)

School of Physics and Opto-Electronic Engineering, Ludong University, Yantai 264025, *China*

(Received 16 December 2020; revised manuscript received 27 January 2021; accepted manuscript online 29 January 2021)

Using the evolutionary methodology for crystal structure prediction, we have predicted the orthorhombic *Cmcm* and *Pnma* phases for ScB_4. The earlier proposed CrB_4-, FeB_4-, MnB_4-, and ReP_4-type structures for ScB_4 are excluded. It is first discovered that the *Cmcm* phase transforms to the *Pnma* phase at about 18 GPa. Moreover, both phases are dynamically and mechanically stable. The large bulk modulus, shear modulus, and Young's modulus of the two phases make it an optimistic low compressible material. Moreover, the strong covalent bonding nature of ScB_4 is confirmed by the ELF analysis. The strong covalent bonding contributes greatly to its stability.

Keywords: first-principles calculations, high pressure, transition metal borides

PACS: 61.50.Ah, 61.50.Ks, 61.66.Fn **DOI:** 10.1088/1674-1056/abe116

1. Introduction

Superhard materials are broadly useful in scientific research and industrial applications such as cutting instruments and hard coating, due to their superior properties in high thermal conduction, chemical stability, and high strength. The superhard materials usually exist in those strongly bonded materials formed by light elements, such as diamond, c-BN, B_6O, BC_5, and BC_2N.[1–7] These compounds typically have a high density of electrons and strong covalent bonds. Unfortunately, these compounds are rare and expensive, which can only be produced under extremely high-pressure and high-temperature environments. Several attempts have been made to develop new hard materials. Recent evidence suggests that the incorporation of boride, carbide, nitride, and oxide into heavy transition metals (TMs) is a strong candidate for the design of modern hard materials, such as ReB_2, OsB_2, RuO_2, and WB_4.[8–12] The incorporation of light elements increases the stability of the transition metal by forming a strong covalent linkage between the TM and the light elements. These compounds have been successfully synthesized under ambient or high pressure, and they usually have large bulk and shear moduli. These groundbreaking studies, therefore, open up a new avenue for producing superhard materials.

Recent work has established that 3d-series transition metal tetraborides usually have an unusual three-dimensional framework of interconnected rhombic B_4 units. In these compounds, CrB_4 with a hardness of 48 GPa under environmental pressure conditions was confirmed to be superhard.[13] MnB_4 has a high mechanical performance, with the Vickers hardness to be as high as 40.1 GPa.[14] Besides, Gou *et al.* reported the successful synthesis of FeB_4 experimentally.[15] In this study, FeB_4 was said to have a hardness of up to 62(5) GPa. In a subsequent study, in various analytical models, Zhang *et al.* have stated that FeB_4's Vickers hardness is between 11.7 and 32.3 GPa.[16] Therefore, 3d-series transition metal tetraborides are considered as one of the ideal materials for the design and synthesis of novel superhard materials. In the Sc-B systems, ScB_2, ScB_{12}, ScB_{15}, and ScB_{19} have been studied in experiments.[17–20] Among them, ScB_2 takes the hexagonal structure (No. 191, $P6/mmm$). For ScB_{12}, cubic structure (No. 225, Fm-$3m$) and tetragonal structure (No. 139, $I4/mmm$) have been studied. The crystal structure of ScB_{15} belongs to the tetragonal structure (No. 76, $P4_1$). Besides, ScB_{19} belongs to the tetragonal structure ($P4_12_12$ or $P4_32_12$). In 2019, Bai *et al.* published a paper in which they described that ScB_3 is a monoclinic $C2/m$ structure with a hardness of 37.1 GPa.[21] However, there are no theoretical or experimental reports on ScB_4 up to now. To our knowledge, the determination of crystal structure is essential for understanding its physical properties. ScB_4's uncertainty of the ground state and high-pressure phases contributes to the presence of exotic physical actions. Therefore, resolving the crystal structure of ScB_4 at ambient conditions and high pressure has an important significance.

In this study, the crystal structures, mechanical, and electronic properties of ScB_4 are systematically explored within a wide range of conditions (0–100 GPa) by using first-principles calculations on crystal structure prediction. An orthorhombic *Cmcm* phase has been uncovered for ScB_4. The *Cmcm* phase is

*Project supported by the Young Scientists Fund of the National Natural Science Foundation of China (Grant Nos. 11704170 and 61705097) and the Natural Science Foundation of Shandong Province, China (Grant Nos. ZR2016AP02 and ZR2016EMP01).

†Corresponding author. E-mail: chubinhua0125@126.com

© 2021 Chinese Physical Society and IOP Publishing Ltd

much more stable energetically than the previously proposed CrB_4-, FeB_4-, MnB_4-, and ReP_4-type structures at ambient pressure. But at high pressure, the *Pnma* phase is more stable. Then the structural property, structural stability, mechanical, dynamic, and electronic properties for the new phases are studied by first-principles.

2. Computational detail

In this work, we use the developed crystal structure prediction method by the CALYPSO to search the potential crystal structures of ScB_4 at ambient pressure.[22–24] The structure relaxation is performed in the Vienna *ab initio* simulation package (VASP) code.[25–27] The exchange–correlation functional is treated by the generalized gradient approximation (GGA) with the projector-augmented wave (PAW) potential.[28,29] The $2s^2 2p^1$ and $3p^6 3d^1 4s^2$ are separately selected as the valence electrons for the B and Sc atoms. The k-point samplings in the Brillouin zone are performed using the Monkhorst–Pack scheme with a grid density of $0.03 \times 2\pi$ Å^{-1} employed in the Brillouin zone integration. The formation enthalpy of Sc_mB_n is determined by the equation $\Delta H = H(Sc_mB_n) - mH(Sc) - nH(B)$, where the Sc element from its hexagonal phase and α-B (0–19 GPa), γ-B (19–89 GPa), and α-Ga phase (89–100 GPa) are used to be the referenced phases.[30] The phonon spectra are carried out by drawing the supercell approach as performed in the PHONOPY software package.[31,32] To further verify the mechanical stability of these polymorphs, the elastic constants are calculated with the strain–stress method. Besides, the bulk modulus B and the shear modulus G are estimated via the Voigt–Reuss–Hill approximation by using the obtained elastic constants C_{ij}.[33,34] Young modulus and Poisson ratio are calculated in accordance with the formulas $Y = 9GB/(3B+G)$ and $v = (3B-2G)/(6B+2G)$. The theoretical Vicker's hardness is estimated by the Chen model.[35] The details of convergence tests have been described elsewhere.[36–38]

3. Results and discussion

By employing the crystal structure prediction of the CALYPSO code at ambient pressure, a new orthorhombic *Cmcm* structure for ScB_4 is predicted successfully. The orthorhombic *Cmcm* structure includes four ScB_4 in a unit cell, with the equilibrium lattice parameters of $a = 5.392$ Å, $b = 3.158$ Å, $c = 10.194$ Å, $\alpha = \beta = \gamma = 90°$ under ambient pressure. There are two inequivalent atom positions in *Cmcm*-ScB_4. Sc atoms occupy the Wyckoff positions 4c (0, 0.9025,1.25), and B atoms occupy the Wyckoff positions 16h (−0.8298, 0.6328,0.9221). Each Sc atom in *Cmcm*-ScB_4 is surrounded by twelve boron atoms, which is similar to that in ScB_3 (ScB_{12}, shown in Fig. 1(b)). The polyhedral view of this structure (Fig. 1(a)) reveals the fascinating B–Sc–B sandwiches stacking order along the c-axis. At high pressure, we find a unique orthorhombic structure with the *Pnma* phase to be most stable. At 20 GPa, the optimized lattice constants are $a = 7.035$ Å, $b = 2.944$ Å, $c = 7.408$ Å, $\alpha = \beta = \gamma = 90°$, which is shown in Fig. 1(c).

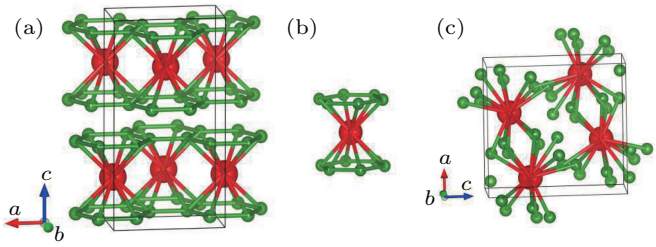


Fig. 1. The crystal structure of the predicted *Cmcm*-ScB_4 and *Pnma*-ScB_4. Large and small spheres represent Sc and B atoms.

We also measure the formation enthalpies of the considered structures of ScB_4 from 0 GPa to 100 GPa. For comparison, CrB_4 (No. 71, *Immm*), FeB_4 (No. 58, *Pnnm*), MnB_4 (No. 14, $P2_1/c$), and ReP_4 (No. 61, *Pbca*) are also considered as the potential phases for ScB_4, hereafter defined as CrB_4-, FeB_4-, MnB_4-, and ReP_4-type structures. The formation enthalpy of ScB_4 is calculated by the formula $\Delta H = H(ScB_4) - H(Sc) - 4H(B)$. Figure 2 presents the formation enthalpy of six phases as a feature of pressure for ScB_4, and it can be clearly seen that the predicted *Cmcm* structure is energetically more favorable than the other structures at ambient pressure. As the pressure increases, the *Pnma* phase becomes the most stable when the pressure is higher than about 18 GPa.

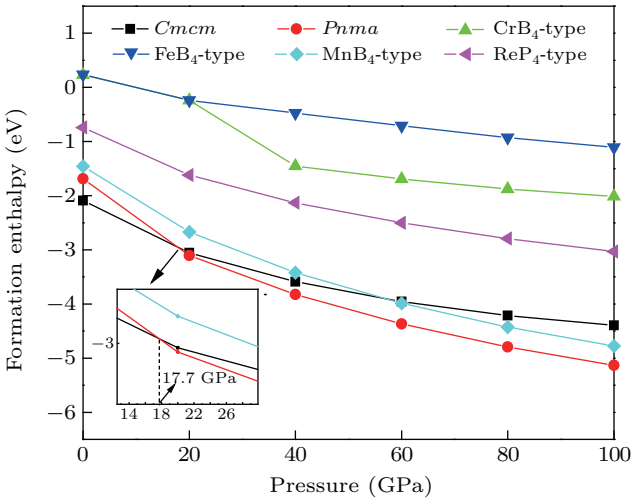


Fig. 2. The formation enthalpy–pressure diagrams for ScB_4 with six different structures.

In order to find the relative stabilities between the two phases and other scandium borides, the relative enthalpy-pressure diagrams were plotted. We choose ScB_2 (space group: $P6/mmm$) and ScB_{12} (space group: $Fm\text{-}3m$) as the competing phases in our calculations. It can be seen from Fig. 3 that the competing phase ScB_2+ScB_{12} is more stable than others at low pressure. When the pressure is increased to 38 GPa, the predicted *Pnma* phase becomes the most stable phase.

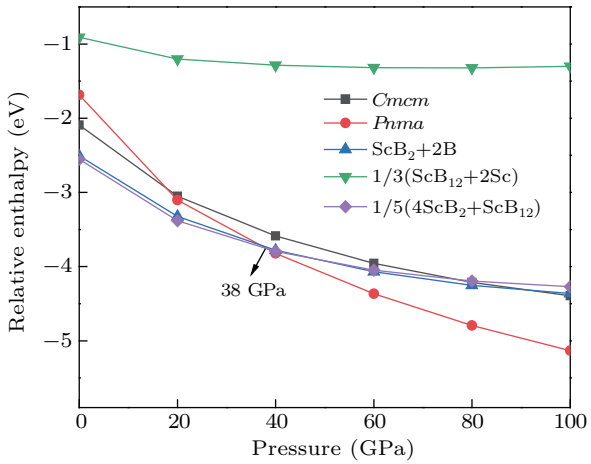


Fig. 3. The relative enthalpy–pressure curve of the *Cmcm* and *Pnma* phases with its respective competing phases.

The convex hull plots of the Sc-B system at the selected pressures are constructed in Fig. 4. As we know, a compound with a formation enthalpy lying on the convex hull is thermodynamically stable. We can expect that this compound can be synthesized in the experiment at their stable pressures. In comparison, the unstable or metastable stoichiometries are above the convex hull. The convex hull of Sc-B compounds at different pressures is performed, which is shown in Fig. 4. Here we choose ScB_2 (space group: $P6/mmm$) and ScB_{12} (space group: $Fm\text{-}3m$) as the competing phases in our calculations. Note that ScB_{15} and ScB_{19} are not considered here due to the large size of the intercalated structures, although these two compounds have been reported experimentally.[39,40] From Fig. 4(a), we can find that all enthalpies of the formation of the three compounds are negative. They are all stable against all decomposition reactions into the pure elements. For *Cmcm*-ScB_4, it does not locate at the convex hull's strong curve, indicating it is unstable and is going to decompose under ambient pressure. In Fig. 4(b), the proposed *Pnma*-ScB_4 phase lies right on the convex hull. Through the above discussion, we can conclude that the *Pnma* phase becomes the ground state beyond 38 GPa.

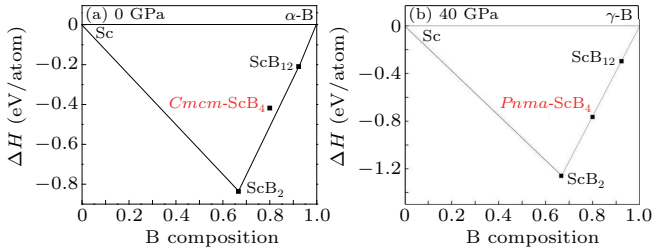


Fig. 4. The convex hulls of ScB_4 at the pressure of (a) 0 GPa and (b) 40 GPa. The solid line denotes the convex hull.

Dynamical stabilities are an important indicator of the existence of structures. We performed the phonon dispersion calculations for *Cmcm*-ScB_4 in 0 GPa and *Pnma*-ScB_4 structures at 20 GPa and 40 GPa (Fig. 5). As can be seen from Fig. 5, no imaginary phonon frequency was found in the Brillouin zone of *Cmcm*-ScB_4 and *Pnma*-ScB_4 structures, indicating that they are dynamically stable.

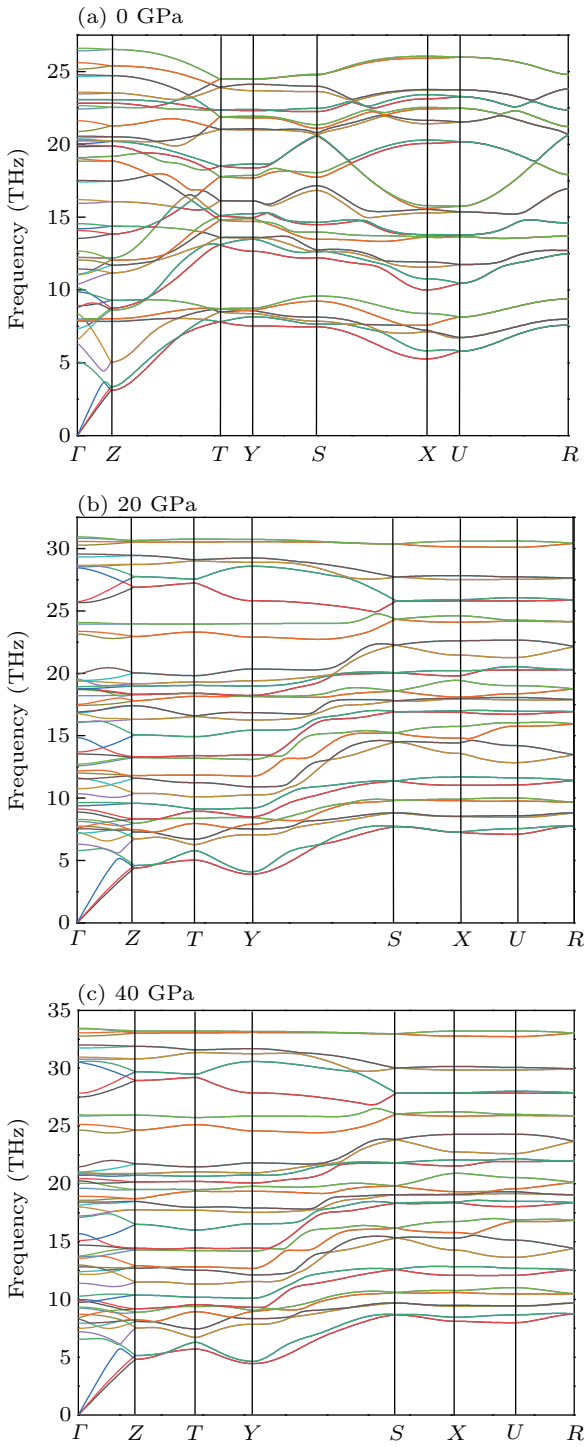


Fig. 5. Phonon dispersion curves of *Cmcm* ScB_4 at (a) 0 GPa, (b) *Pnma* ScB_4 at 20 GPa, (c) *Pnma* ScB_4 at 40 GPa.

To investigate the elastic stability of *Cmcm* and *Pnma* phases for ScB_4, we calculated its elastic constants using the stress-strain method. Table 1 lists the calculated elastic constants of the two phases, also together with the results of other transition terborides. For comparison, the previously reported elastic constants of TMB_4 (TM = Cr, Fe, Mn, Y, Hf) are also

considered in this paper. For an orthorhombic crystal, the independent elastic stiffness tensor consists of nine components of C_{11}, C_{22}, C_{33}, C_{44}, C_{55}, C_{66}, C_{12}, C_{13}, and C_{23}. The mechanical stability is based on the following:

$$C_{11}>0,\quad C_{22}>0,\quad C_{33}>0,\quad C_{44}>0,\quad C_{55}>0,\quad C_{66}>0,$$
$$C_{11}+C_{22}+C_{33}+2(C_{12}+C_{13}+C_{23})>0,$$
$$C_{11}+C_{22}-2C_{12}>0,$$
$$C_{11}+C_{33}-2C_{13}>0,$$
$$C_{22}+C_{33}-2C_{23}>0.$$

From Table 1, we can verify that C_{ij} of *Cmcm* and *Pnma* phases meet the above stability criteria, indicating that they are all mechanically stable. So that, ScB_4 is both mechanically and dynamically stable at ambient pressure and high pressure. For *Cmcm*-ScB_4, the values of calculated C_{33} are a lot lower than those of C_{11} and C_{22}, indicating that the bonding strength along the [001] direction is far softer than that along the [100] and [010] directions. Meanwhile, compared to the *c*-axis, *Cmcm*-ScB_4 is difficult to compress along the *a* and *b* axes. But in *Pnma*-ScB_4, the values of calculated C_{11} are a lot lower than those of C_{22} and C_{33}, indicating that it is difficult to compress along the *b* and *c* axes. Sadly, no experimental data is available for comparison. Our findings may therefore be a guideline for future studies and applications of 3d transition metal borides under high pressures. Accurate elastic constants are helpful to understand the mechanical properties and provide beneficial information to estimate the properties of a material. ScB_4 has the bulk modulus of 204 GPa and 284 GPa for *Cmcm* and *Pnma* phases, which are larger than that of the YB_4. The shear modulus of a material is well known to measure its resistance to shear deformation. The calculated shear module of *Cmcm*- and *Pnma*-ScB_4 are 184 and 217 GPa, respectively, which are close to that of FeB_4. It is expected that they can withstand the shear strain to a large extent. The results of Young's modulus and Poisson's ratio are given in Table 1. The large Young's moduli values of *Cmcm* and *Pnma*-ScB_4 (424 and 519, respectively) indicate its strong capability of resisting tension and pressure in the range of elastic deformation. Poisson's ratio indicates that the relative direction of material bonding has an important influence on the hardness of the material. For covalent materials, the usual value v is 0.1, and for metal materials, 0.33. Among these compounds, *Cmcm*-ScB_4 has the v of 0.153 and *Pnma*-ScB_4 has the v of 0.196, which suggests a degree of covalent bonding for both phases. The G/B ratio indicates the ductility or brittleness of a material, G/B less than 0.57 means the material is ductile, otherwise brittle. The calculated G/B ratio of *Cmcm*- and *Pnma*-ScB_4 is implying its brittle nature. All of these excellent mechanical properties strongly suggest that ScB_4 is a potential candidate to be incompressible and hard materials. The hardness of materials can be measured using an empiric formula $H_v = 2(K^2G)^{0.585} - 3$ where $K = G/B$ denotes the Pugh's modulus ratio. Using this model, we calculate the hardness of *Cmcm*- and *Pnma*-ScB_4 to be 34.5 GPa and 31 GPa, respectively. We also note that the order of hardness value for the structures considered here is concluded as follows: YB_4 (17.04 GPa) < FeB_4 (24.2 GPa) < *Pnma*-ScB_4 (31 GPa) < *Cmcm*-ScB_4 (34.5 GPa) < MnB_4 (38.7 GPa) < CrB_4 (45.1 GPa) < HfB_4 (45.7 GPa). This result suggests that ScB_4 has low mechanical strength and does not become a superhard material. Because of the high boron concentration, 3D boron networks are not expected to enhance the strength of ScB_4. Therefore, ScB_4 is expected to have mechanical properties consistent with those of other transition metal borides. Of course, these properties need further theoretical and experimental studies.

Table 1. The calculated elastic constants C_{ij} (GPa), bulk modulus B (GPa), shear modulus G (GPa), Young's modulus Y (GPa), G/B, Poisson's ratio v, and hardness H_v (GPa) for ScB_4 in comparison with available theoretical results.

Structure	Ref.	C_{11}	C_{22}	C_{33}	C_{44}	C_{55}	C_{66}	C_{12}	C_{13}	C_{23}	B	G	Y	G/B	v	H_v
Cmcm-ScB_4	this work	497	546	363	161	164	217	36	107	76	204	184	424	0.902	0.153	34.5
Pnma-ScB_4	this work	567	687	616	241	210	150	86	150	149	284	217	519	0.764	0.196	31
Immm-CrB_4	theor.[a]	591	931	467	252	280	225	64	115	97	275	259		0.942	0.142	45.1
	theor.[b]	586	942	519	251	282	227	66	133		290	296		1.02	0.119	
Pnnm-FeB_4	theor.[c]	408	754	448	219	141	229	165	160	154	277	186	456	0.671	0.226	
	theor.[d]	405	749	479	218	177	225	142	152	129	263	199	476	0.755	0.198	
	theor.[a]	381	710	435	218	114	227	137	143	128	253	177		0.697	0.216	24.2
$P2_1/c$-MnB_4	theor.[e]	522	872	524	234	193	222	90	86	96	266	235	544		0.159	38.7
$P4/mbm$-YB_4	theor.[f]	454		442	108		132	80	33		182	144	342	0.791	0.18	17.04
Cmcm-HfB_4	theor.[g]	606	611	505	251	197	264	53	83	99	243	240	542	0.987	0.128	45.7

[a]Ref. [13], [b]Ref. [41], [c]Ref. [42], [d]Ref. [43], [e]Ref. [44], [f]Ref. [45], [g]Ref. [46].

To understand the mechanical properties of ScB_4, the total and partial densit of states of *Cmcm*-ScB_4 and *Pnma*-ScB_4 were calculated, shown in Fig. 6. These two phases show similar metallic features because of finite DOS at the Fermi level. As seen from Fig. 6(a), we can find that in the region from 15.2 to −6.5 eV, the contributions are primarily contributed

by the B-2s and B-2p orbitals with slight contributions of Sc-3d. From −6.5 eV to the E_F, B-2p orbitals mostly contribute to the DOS. In Fig. 6(b), there is no clear overlap of B-2p and Sc-3d electron in the range of −16.5 and 0.7 eV. As seen from Fig. 6, there is a deep valley, namely, a pseudogap of DOS, which is the borderline between the bonding and antibonding states. The presence of pseudogap will increase the structural stability of ScB_4.

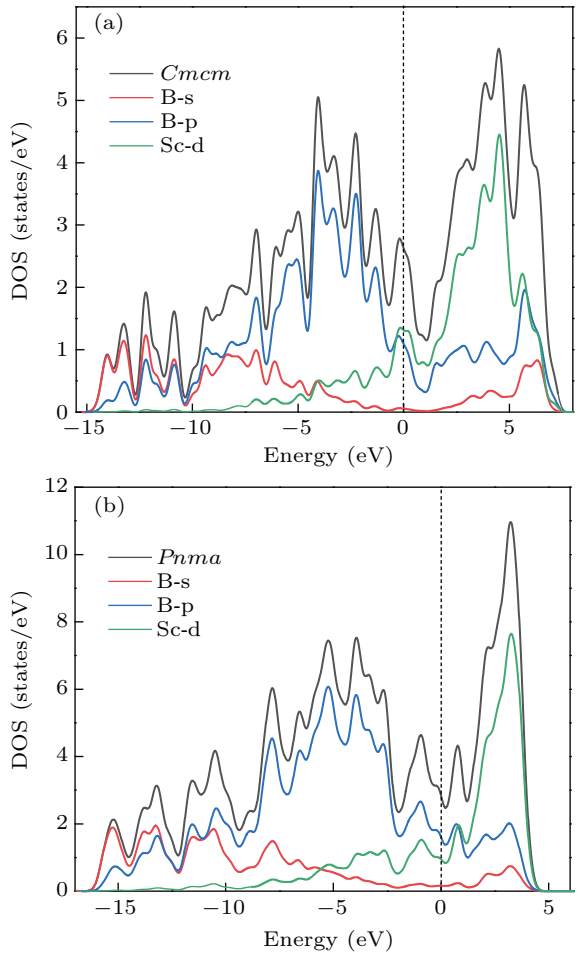


Fig. 6. Total and partial densit of states for (a) *Cmcm*-ScB_4 and (b) *Pnma*-ScB_4.

The electronic localization function (ELF) is widely used to describe and visualize chemical bonding. The ELF is a contour chart in real space with values ranging from 0 to 1. In general, ELF = 1 indicates the localized features of covalent bonds or lone pairs, ELF = 0.5 indicates the probability of electron-like gas pairs, and ELF = 0 indicates a completely off-domain. We plotted the contours of ELF = 0.75 and (001) plane for *Cmcm*-ScB_4 in Fig. 7(a), we can see six-membered ring layers of *Cmcm*-ScB_4. High electron localization between B atoms can be observed, suggesting strong covalent B–B bonds. Besides, we also plotted the (102) plane for *Cmcm*-ScB_4in Fig. 7(b), and there is a strong Sc–B covalent bonding in the *Cmcm*-ScB_4, which is a weaker chemical bond than the B–B bond. The strong B–B and Sc–B covalent bonds contribute significantly to hardness and structural stability.

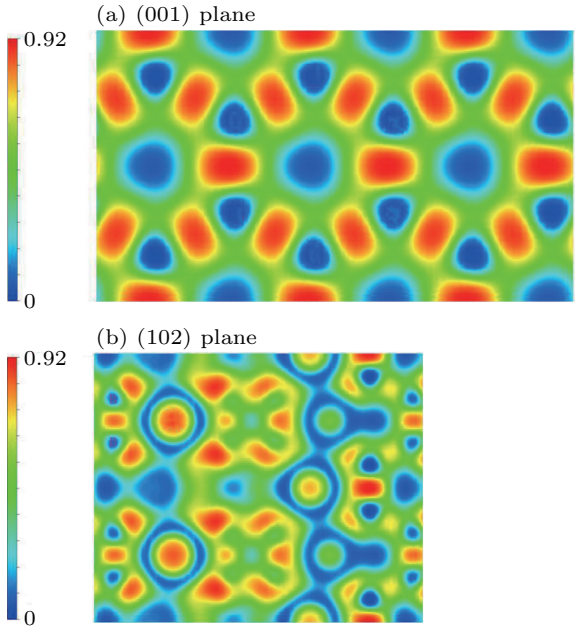


Fig. 7. The contours of the electronic localization function of the *Cmcm*-ScB_4 on the (001) plane (a) and (102) plane (b).

4. Conclusion

In summary, we have predicted two novel boron-rich ScB_4 with orthorhombic *Cmcm* space group at ambient pressure and *Pnma* space group at high pressure through the PSO technique. In the meantime, the structural properties, phase stability, mechanical strength, and electronic properties of the two phases have been systematically investigated in the first-principles calculations. It is illustrated that the predicted two phases are dynamically and elastically stable. The calculated hardness of the *Cmcm* phase is 34.5 GPa, which is a potential hard material. Moreover, the electronic localization function analysis has demonstrated that the strong covalent B–B and Sc–B bonding play a key role in the incompressibility and hardness of ScB_4. We look forward to furthering high-pressure work on the synthesis of the superhard material.

References

[1] Occelli F, Farber D L and Toullec R L 2003 *Nat. Mater.* **2** 151
[2] Zheng J C 2005 *Phys. Rev. B* **72** 052105
[3] Zhang Y, Sun H and Chen C F 2006 *Phys. Rev. B* **73** 144115
[4] Solozhenko V L, Andrault D, Fiquet G, Mezouar M and Rubie D C 2001 *Appl. Phys. Lett.* **78** 1385
[5] Zhang Y, Sun H and Chen C 2004 *Phys. Rev. Lett.* **93** 195504
[6] Solozhenko V L, Kurakevych O O, Andrault D, Godec Y L and Mezouar M 2009 *Phys. Rev. Lett.* **102** 015506
[7] He D W, Zhao Y S, Daemen L, Qian J, Shen T D and Zerda T W 2002 *Appl. Phys. Lett.* **81** 643
[8] Chung H Y, Weinberger M B, Levine J B, Kavner A, Yang J M, Tolbert S H and Kaner R B 2007 *Science* **316** 436
[9] Chung H Y, Weinberger M B, Yang J M, Tolbert S H and Kaner R B 2008 *Appl. Phys. Lett.* **92** 261904
[10] Cumberland R W, Weinberger M B, Gilman J J, Clark S M, Tolbert S H and Kaner R B 2005 *J. Am. Chem. Soc.* **127** 7264
[11] Tse J S, Klug D D, Uehara K, Li Z Q, Haines J and Léger J M 2000 *Phys. Rev. B* **61** 10029
[12] Gu Q F, Krauss G and Steurer W 2008 *Adv. Mater.* **20** 3620

[13] Niu H Y, Wang J Q, Chen X Q, Li D Z, Li Y Y, Lazar P, Podloucky R and Kolmogorov A N 2012 *Phys. Rev. B* **85** 144116
[14] Gou H Y, Li Z P, Niu H, Gao F M, Zhang J W, Ewing R C and Lian J 2012 *Appl. Phys. Lett.* **100** 111907
[15] Gou H Y, Dubrovinskaia N, Bykova E, Tsirlin A A, Kasinathan D, Schnelle W, Richter A, Merlini M, Hanfland M and Abakumov A M 2013 *Phys. Rev. Lett.* **111** 157002
[16] Zhang M, Lu M C, Du Y H, Gao L L, Lu C and Liu H Y 2014 *J. Chem. Phys.* **140** 174505
[17] Levchenko G, Lyashchenko A, Baumer V, Evdokimova A, Filippov V, Paderno Y and Shitsevalova N 2006 *J. Solid State Chem.* **179** 2949
[18] Przybylska M, Reddoch A H and Ritter G J 1963 *J. Am. Chem. Soc.* **85** 407
[19] Pediaditakis A, Haseloff S and Hillebrecht H 2011 *Solid State Sci.* **13** 1465
[20] Tanaka T, Okada S and Gurin V N 1998 *J. Alloys Compd.* **267** 211
[21] Bai T T, Zhang G T, Zhao Y R, Chen L, Mu B X, Han Y F and Wei Q 2019 *Mol. Phys.* **118** e1603411
[22] Wang Y C, Lv J, Zhu L and Ma Y M 2010 *Phys. Rev. B* **82** 094116
[23] Wang Y C, Lv J, Zhu L and Ma Y M 2012 *Comput. Phys. Commun.* **183** 2063
[24] Wang Y C, Lv J, Zhu L, Lu S H, Yin K T, Li Q, Wang H, Zhang L J and Ma Y M 2015 *J. Phys.: Condens. Matter* **27** 203203
[25] Kresse G and Hafner J 1993 *Phys. Rev. B* **47** 558
[26] Kresse G and Hafner J 1994 *J. Phys.: Condens. Matter* **6** 8245
[27] Kresse G and Furthmüller J 1996 *Phys. Rev. B* **54** 11169
[28] Perdew J P, Burke K and Ernzerhof M 1996 *Phys. Rev. Lett.* **77** 3865
[29] Kresse G and Joubert D 1999 *Phys. Rev. B* **59** 1758
[30] Will G and Kiefer B 2001 *Z. Allg. Chem.* **627** 2100
[31] Togo A, Oba F and Tanaka I 2008 *Phys. Rev. B* **78** 134106
[32] Togo A and Tanaka I 2015 *Scr. Mater.* **108** 1
[33] Reuss A 1929 *Z. Angew. Math. Mech.* **9** 49
[34] Hill R 1952 *Proc. Phys. Soc. London* **65** 394
[35] Chen X Q, Niu H, Li D and Li Y 2011 *Intermetallics* **19** 1275
[36] Wang Y C, Tian F B, Li D, Duan D F, Xie H, Liu B B, Zhou Q and Cui T 2019 *Chin. Phys. B* **28** 56104
[37] Zhang D, Jin X L, Zhuang Q, Li Y, Yang S H, Song L Y, Liu B B and Cui T 2019 *Chin. Phys. B* **28** 56101
[38] Lu M Y, Huang Y P, Tian F B, Li D, Duan D F, Zhou Q and Cui T 2020 *Chin. Phys. B* **29** 53104
[39] Pediaditakis A, Haseloff S and Hillebrecht H 2011 *Solid State Sci.* **13** 1465
[40] Tanaka T, Okada S and Gurin V N 1998 *J. Alloys Compd.* **267** 211
[41] Xu H B, Wang Y X and Lo V C 2011 *Phys. Status Solidi RRL* **5** 13
[42] Zhang X Y, Qin J Q, Ning J L, Ning X W, Sun X T, Li M Z, Ma R P and Liu J 2013 *J. Appl. Phys.* **114** 183517
[43] Zhang M G and Yan H Y 2014 *Solid State Commun.* **187** 53
[44] Yang M, Wang Y C, Yao J L, Li Z P, Zhang J, Wu L L, Li H, Zhang J W and Gou H Y 2014 *J. Solid State Chem.* **213** 52
[45] Fu Y Y, Li Y W and Huang H M 2014 *Chin. Phys. Lett.* **31** 116201
[46] Zhang G T, Gao R, Zhao Y R, Bai T T and Hu Y F 2017 *J. Alloys Compd.* **723** 802